DEVELOPMENT OF HIGH PERFORMANCE MULTICRYSTALLINE SILICON WITH CONTROLLED SEEDING

A. Hess, P. Krenckel, T. Trötschler, T. Fehrenbach, S. Riepe
Fraunhofer Institute for Solar Energy Systems ISE
Heidenhofstrasse 2, D- 79110 Freiburg, Germany
Phone +49 761 4588-5644, adam.hess@ise.fraunhofer.de

ABSTRACT: High Performance multicrystalline silicon ingots are mostly produced with seeded growth on small size silicon material, which determines the beneficial initial grain structure and orientations of the crystallites. A drawback of this approach is the increased area of low minority charge carrier lifetime in the lower part of the ingot and thus a worse yield. Also, the solidification process time is increased as the seed has to remain solid in a well controlled manner. Both drawbacks can be addressed by using a thin seeding layer on the crucible bottom, which has a higher melting point than silicon. The area of low minority carrier lifetime at the ingot bottom is comparable to standard multicrystalline silicon, whereas the crystal structure is significantly improved. Several seeding layer configurations were investigated and SiO_2 with different grain sizes was chosen for G1-sized experiments. The resulting brick shows a grain and defect structure close to the High Performance multicrystalline silicon reference while reducing the width of the impurity indiffusion zone in the bottom. By optimizing the seeding layer in conjunction with the thermal process, a higher yield of high quality material is possible.
Keywords: Crystallization, Silicon, SiO_2, High Performance, Multicrystalline

1 INTRODUCTION

Wafer from multicrystalline silicon (mc-Si) are still the basis for approx. 50% of all sold solar cells [1]. In this fraction, the role of High Performance multicrystalline silicon (HP mc-Si) is dominating [2-3]. Due to the characteristic homogeneous and small grain structure with random orientations, dislocation creation is suppressed and induced ones tend to annihilate at random angle grain boundaries [4]. Thus, material quality limiting crystal defects can be reduced. But for this, the seed material has to remain solid during melting, leading to longer process times compared to standard mc-Si growth. Also, due to the seed preservation, the ingot yield is smaller as a bigger portion of the bottom part can`t be used.

This work aims at the development of HP mc-Si ingots with low dislocation densities and optimized material quality based on the use of a thin seeding layer. In this approach, the standard mc-Si solidification process can be used leading to the improved material quality of HP mc-Si. Similar approaches have been tested with promising results [5-7], although most ones used an additional Si_3N_4-coating on top of the layers. Our experiments showed that for some seeding materials a Si_3N_4-coating leads to worse results than without. For that we used SiO_2-powder as a direct seeding layer with specific grain sizes to study their influence on the grain structure and the material quality of a resulting G1-ingot.

2 EXPERIMENTAL

In this work, we investigated the influence of different coatings as seeding layer for HP mc-Si growth. On small scale (G0, 800 g Si) various materials have been tested as nucleation layer with and without coatings on top. The samples have been prepared and analyzed for initial grain size, grain size homogeneity and evolution. SiO_2-powder without a coating was identified as best candidate for G1-experiments.
SiO_2-powders with a variation of initial particle size are used. The ingots were grown in a G1-sized crucible. Four ingots with 14.0 kg of high purity silicon feedstock were crystallized in a laboratory Vertical Gradient Freeze furnace (PVA TePla VGF632). The ingots were p-doped with boron for a target resistivity of 0.5 - 1.5 Ωcm.
We used an in-house developed, non-standard coating for the experiments (ISE coating) with and without nucleation layer and a standard industrial coating for a reference ingot without seed and one on granular Si.

The crucible bottom was covered with a 1 mm thick layer of high quality SiO_2-powders from two sizes, quartzpowder with a grain size distribution of 75-300 µm (Powder 1) on the left half and with 37-63 µm (Powder 2) on the right half (Figure 1). As a comparison a standard mc-ingot was grown with the same thermal process. Both materials have been compared with a reference HP mc-Si material grown on granular Si. For seed preservation, a different thermal process had to be applied.

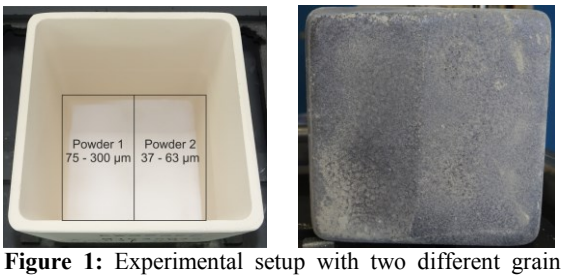

Figure 1: Experimental setup with two different grain size distributions on every half of the G1-sized crucible bottom (75 - 300 µm left and 37 - 63 µm right) and the bottom of the resulting Si-ingot.

A central brick with 156 mm edge length was prepared and analyzed for inclusions and brick minority carrier lifetime as well as electrical resistivity. Inclusions and other particles were identified using the Intego Orion HighRes IR block inspection system. Lifetime and electrical resistivity measurements were done with the Semilab WT-2000D. Fourier-transform Infrared Spectroscopy (FTIR) measurements were performed to identify oxygen concentrations using the Vertex 80v in combination with the Hyperion microscope (Bruker). The

concentration of interstitial Oxygen (O_i) was measured every 5 mm along the brick height. For this measurement setup, the samples had to be divided into two parts, resulting in a data gap at 75-80 mm to avoid edge effects.

Wafers were produced from this ingot material by slurry based multi-wire sawing and characterized with respect to grain structure, dislocated area fraction, inclusions and material properties. To visualize the grain structure and the material quality Photoluminescence- (PL) and optical measurements were performed on the wafer using the Hennecke Wafer Inspection System.

3 RESULTS AND DISCUSSION

3.1 Inclusions

In a first step, the sawn bricks were polished and scanned for inclusions by IR inspection. The Intego Orion HighRes IR block inspection system allows a resolution down to 18µm to identify inclusion and other defects in the brick volume. This way, we analyzed if the SiO_2-powder may have been incorporated into the brick. As we used an experimental coating (ISE coating) on the crucibles, these two bricks were compared to a reference brick with standard industrial coating. In Figure 2, the Small Point Defect Density (SPDD) distribution over brick height is shown. There is no significant difference in SPDD in the bricks with and without SiO_2-powder, so the powder does not trigger increased particle inclusion. Whereas, in the brick grown with a standard industrial crucible coating, there are 10 times more small inclusions identified. In this case, the influence by the coating is dominant.

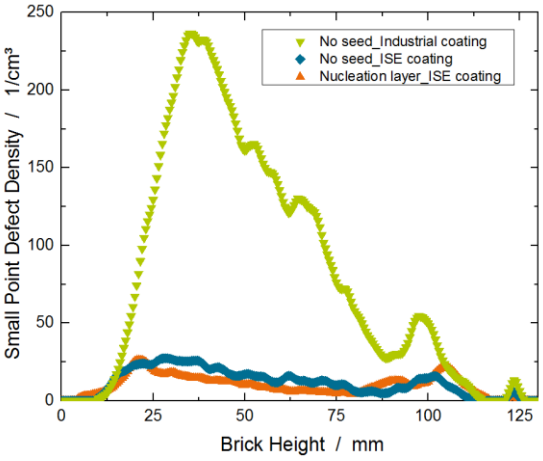

Figure 2: Small Point Defect Density over brick height for three different bricks. There are 10 times more small inclusions in the brick grown in the crucible with a standard industrial coating than the ones with the ISE coating.

3.2 Grain analysis

In Figure 3, we can see optical images of the wafer from three different brick heights (20, 60 and 100 mm). For the HP mc-Si brick grown on granules, the bottom-most wafer is at brick height of 40 mm due to the remained seed layer of 30 mm. It shows the typical small and homogeneous grain distribution. These characteristics and the random grain orientations are the key parameter to reach improved material quality by lowering mechanical stress and thus avoid the occurrence of dislocations. Even when dislocation clusters occur in some grains, they may be overgrown by other grains. This overgrowth is enhanced due to a small and homogeneous grain size distribution. The SiO_2-seeded brick shows a grain structure and size distribution close to the HP mc-Si reference. Although this brick has two different seeding layers, there is no obvious difference visible between the two halves. In the standard mc-Si brick, the undercooling at the start of the crystallization phase was higher. We can clearly see dendritic growth in the initial nucleation phase. As both experiments used the same thermal process, the combination of additional nucleation sites and slightly reduced thermal conductivity by the SiO_2-layer can avoid dendritic growth in this case.

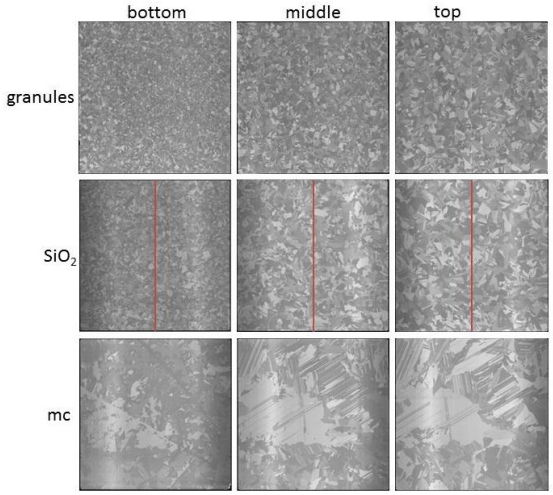

Figure 3: Grain structure evolution of the different bricks at three different heights shown by optical wafer images (156x156 mm²).

To compare the grain structures quantitatively the optical images were recorded and analyzed according to [8]. After a segmentation step the grain distribution is analyzed using a developed algorithm and the grain sizes and homogeneity of the distribution are compared as listed in Table I for the results of the seeding tests on small scale. As the value for mean grain size is dominated by the amount of smallest grains, a much better parameter to describe the grain size is the 50th weighted area percentile (A_{50}). The mean relative difference of the consecutive weighted percentiles showed to be a good measure for the inhomogeneity of the grain size distribution (GAI), where a smaller value means more homogeneity. Further explanations can be found in [8]. This way the best seeding layers were selected after various pretests in smaller crucibles, where SiO_2-powder without a Si_3N_4-capping proved to be the best option.

Table I: Grain analysis comparison of the bottom-most wafer of each brick from the small seeding tests using the procedure presented in [8]. 50th weighted area percentile (A_{50}), the mean relative difference of the consecutive weighted percentiles (GAI) are shown for experiments on SiO_2-powders with and without Si_3N_4-capping.

	Powder 1	Powder 1 + C	Powder 2	Powder 2 + C
A_{50} [mm^2]	3.99	41.42	4.48	25.59
GAI	0.88	0.63	0.83	0.61

The evolution of the grain size over brick height can be found in Figure 4 and the initial values for the bottom-most wafer in Table II.

Table II: Grain analysis comparison of the bottom-most wafer of each brick using the procedure presented in [8]. 50th weighted area percentile (A_{50}), the mean relative difference of the consecutive weighted percentiles (GAI) are shown for experiments on granules, with SiO_2-powders, and without seeding layer.

	Granules	Powder 1	Powder 2	mc
A_{50} [mm²]	1.44	3.50	3.78	66.91
GAI	0.51	0.46	0.44	1.41

The granular seeded brick shows the smallest grain distribution and a linear growth of the median over brick height. The SiO_2-seeded brick shows the same distribution and growth on both sides. Regarding initial grain size and grain size evolution, there is no difference between the two SiO_2-powders. The increase corresponds to the granules-seeded brick, but the overall median sizes are about 2 mm² smaller at the same height above the seeding position as the granules remain on the bottom of the crucible. The mc-brick with dendritic seeding has much bigger grains and a high inhomogeneity, too. Overall, the median stays at a value about 70 mm².

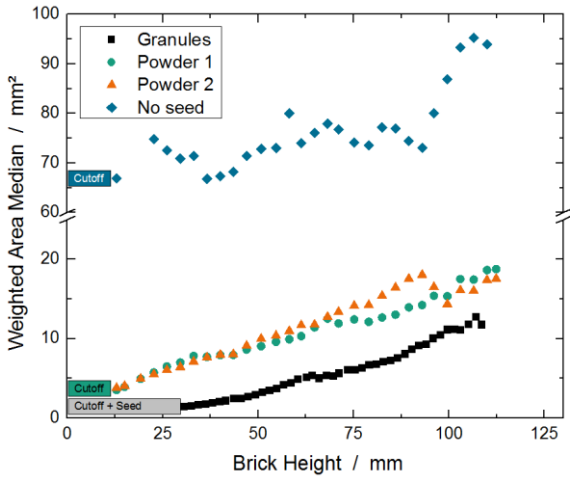

Figure 4: Weighted area median over brick height for the three bricks. The grain structure in the SiO_2-seeded brick shows a similar evolution like the one grown on granules, being about 2 mm² bigger in size.

3.3 Impurities and dislocations

In Figure 5 two PL-images are shown from the bottom and the top of the grown SiO_2-seeded brick. From bottom to top we can identify two different regions corresponding to the two seeding layers. Both show different effects on the PL-intensity. In the bottom wafer, the right side with Powder 1 as seeding layer shows a reduced PL-signal in the grains while the left one, grown on powder 2, doesn`t. This effect is linked to the width of the indiffusion zone into the brick which is smaller here for the left side. On the other hand the dislocation density is higher on the left side in the middle wafer. However, both sides show the same grain structure and grain size in the bottom part of the brick as seen in Figure 3.

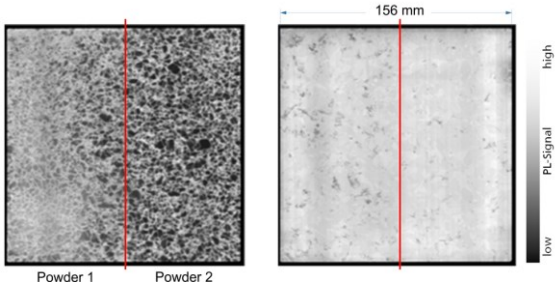

Figure 5: PL images of wafer from 10 mm (left) and 60 mm (right) ingot height. Different seed grain sizes were placed on each half. There is a clear difference in impurity indiffusion area and dislocation density for both sides.

In Figure 6, all wafer PL-images were stacked to create a virtual image of the brick vertical cross section to illustrate the different impurity indiffusion lengths. Bottom and top cutoffs are drawn in as these regions weren`t wafered.

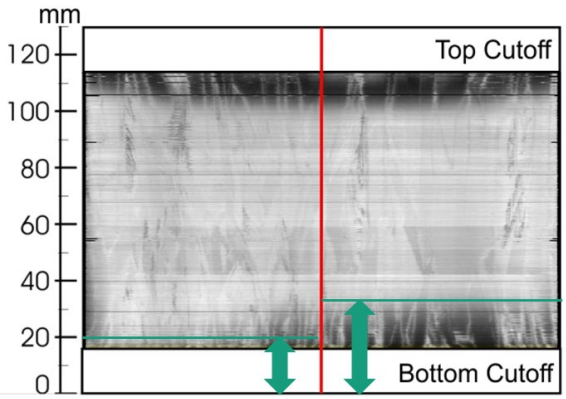

Figure 6: Virtual cross section through the brick using all wafer PL-images. In the bottom part, the different widths of the impurity indiffusion zones for the two seeding layers are indicated. The height was calculated using a PL-intensity threshold.

To characterize this length a certain overall PL-intensity has been defined as threshold. This was done for all bricks and the differences can be seen in Figure 7.

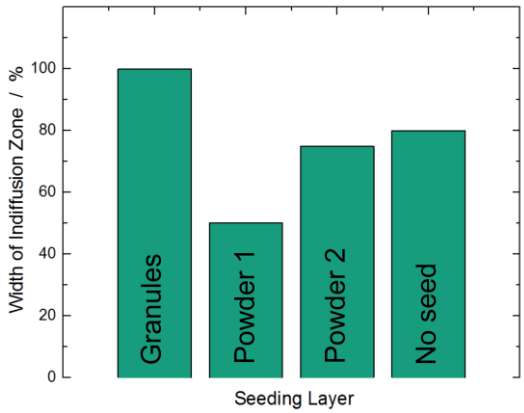

Figure 7: Impurity indiffusion lengths extracted from PL-images for different seeding layers

For the ingot grown on Si granules, this value is higher as the seed remains solid and the process time is increased. For powder 2, the value is comparable to the standard mc-process whereas it`s significantly reduced for the powder 1. The reason is either the SiO_2-material quality itself or an effect as diffusion barrier and has to be validated in further experiments.

The dislocation area fraction was calculated from the PL-images. The results are shown in Figure 8. The dislocation multiplication is high for the mc-material as grains are much bigger and stress relaxation by forming dislocations is common. The material grown on granules stays with only slight variations at 0.5 - 1 area%, which is a typical value for HP mc-Si. For the SiO_2-powder, there is a clear difference between the two grain sizes. On the coarser grains in powder 1, the value stays constant at about 2 area%. But especially on powder 2, dislocation density is reduced and in good agreement with HP mc-Si on granules.

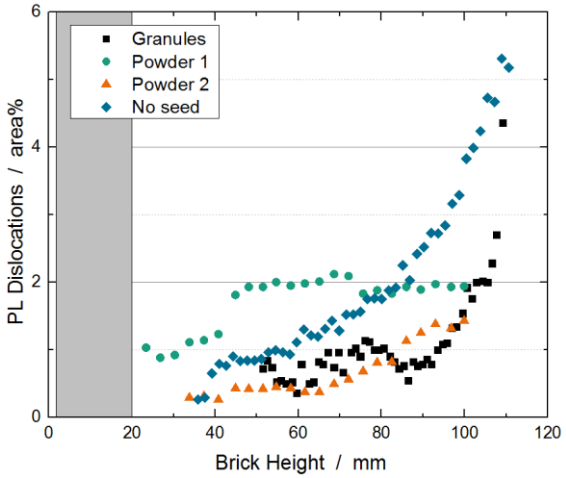

Figure 8: Dislocation area fraction over brick height for the seeded and not seeded bricks calculated from the PL-images. The indiffusion area was not analyzed due to the low PL-intensity.

3.4 Oxygen content

As the silicon melt is in direct contact with the SiO_2-powder, the Oxygen concentration could be a critical parameter. The interstitial Oxygen concentration over brick height is shown in Figure 9. Both curves show similar behavior. Only the first centimeters of the SiO_2-sample shows increased values which rapidly reach the same level at about 20 mm ingot height. Thus, the SiO_2 powder has no obvious negative effect on the O_i-concentration for most of the ingot volume.

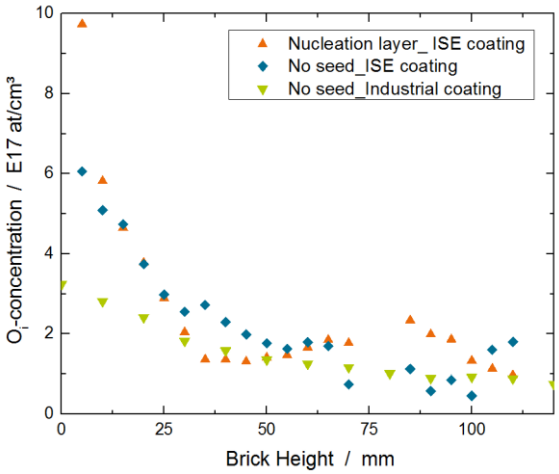

Figure 9: O_i-concentration over brick height; The distribution is comparable, only in the first centimeters the value is slightly higher in the sample with SiO_2-seed.

4 CONCLUSION

Different configurations of materials and particle sizes have been tested in a small crucible setup to identify the most promising candidates to act as a thin seeding layer for HP mc-Si growth in a standard mc-Si solidification process. These results were transferred to grow a G1-sized ingot. A HP mc-Si structure could be achieved with both seed grain sizes used at each ingot half. We also see a positive impact of the material used in PL wafer measurements in regard to lifetime for powder 1 and dislocation density for powder 2. Powder 2 shows a high potential as nucleation layer for HP mc-Si ingots with reduced width of impurity indiffusion zone compared to granular seeds. By optimizing the nucleation layer in conjunction with the thermal process, a higher yield of high quality material should is possible.

5 ACKNOLEDGMENTS

The authors would like to thank Wacker Polysilicon and AlzChem for crystallization materials and all colleagues of the crystallization and characterization teams at Fraunhofer ISE, especially F. Haas and P. Häuber for material processing.

This work was part of a SOLAR-ERA.NET project and was funded by the German Federal Ministry for Economic Affairs and Energy within the research project “HighCast” (grant number 0325894)

6 REFERENCES

[1] N. S. Pujari et al., “International Technology Roadmap for Photovoltaic (ITRPV)”, Ninth Edition 2018, p. 40

[2] Lan, C. W.; Yang, C. F.; Lan, A.; Yang, M.; Yu, A.; Hsu, H. P.; Hsu, B.; Hsu, C., “Engineering silicon crystals for photovoltaics”, CrystEngComm 18 (9) (2016), 1474-1485

[3] Lan, C. W.; Lan, A.; Yang, C. F.; Hsu, H. P.; Yang, M.; Yu, A.; Hsu, B.; Hsu, W. C.; Yang, A., “The emergence of high-performance multi-crystalline silicon in photovoltaics”, Journal of Crystal Growth, vol. 468 (2017), 17-23

[4] G. Stokkan, A. Song, B. Ryningen, “Investigation of the Grain Boundary Character and Dislocation Density of Different Types of High Performance Multicrystalline Silicon”, Crystals 8(9) (2018), 341
[5] Huali Zhang, Da You, Chunlai Huang, Yihua Wu, Yan Xu, Peng Wu, “Growth of multicrystalline silicon ingot with both enhanced quality and yield through quartz seeded method”, Journal of Crystal Growth, vol. 435 (2016), 91–97
[6] Junjing Ding, Yunyang Yu, Wenliang Chen, Xucheng Zhou, Zhiyong Wu, “Effect of the fused quartz particle density on nucleation and grain control of high-performance multicrystalline silicon”, Journal of Crystal Growth, vol. 454 (2016), 186–191
[7] Yu, Yunyang; Ding, Junjing; Chen, Wenliang; Zhang, Zhaoyu; Zhou, Xucheng; Zhong, Genxiang; Huang, Xinming, “Growth of High-Quality Multicrystalline Silicon Ingot through the Cristobalite Seeded Method”, Journal of Materials Science and Engineering B (11-12) (2016), 304-310
[8] T. Strauch, M. Demant, P. Krenckel, S. Riepe, S. Rein, “Analysis of grain structure evolution based on optical measurements of mc Si wafers”, Journal of Crystal Growth, vol. 454 (2016), 147–155